ISSN No:-2456-2165 https://doi.org/10.38124/ijisrt/26sep312

Delayed Ring Closure as the Primary Cause of Tunnel Collapse in Swelling Claystone: A Lesson from Jatigede Hydroelectric Power Project, Indonesia

Kaustubh Mani Nepal[1*]

[1]PT. Prima Layanan Nasional Enjiniring (PLNE), Indonesia.

Corresponding Author: Kaustubh Mani Nepal[1*]

Publication Date: 2026/09/22

Abstract: This paper analyses the severe squeezing behaviour and collapse incidents in the Jatigede Penstock Tunnel in West Java, Indonesia. The 731.54-meter-long steel-lined pressure tunnel passes through highly plastic claystone with a swelling potential of 37% and porosity of 46%. Three major collapse events occurred between Chainage PS0+290 and PS0+298, resulting in invert heaving of up to 600 mm over a 70-meter section and convergence deformations exceeding 771 mm at monitoring stations. Convergence monitoring data from 11 tunnel sections between PS0+253 and PS0+395 were evaluated using Sulem's time-dependent deformation model, revealing three behavioural groups: (a) severe squeezing near the collapse zone, with asymptotic convergences up to 1,421 mm and creep ratios as high as 6.5; (b) moderate creep at varying distances; and (c) limited deformation in more competent ground. The lessons learned from this analysis underscore the critical need for immediate ring closure in squeezing ground, the importance of systematic rock bolting, the effectiveness of real-time monitoring, and the value of customized support systems for managing swelling ground conditions. These findings provide essential insights that will significantly improve tunnel construction practices in similar geological contexts.

Keywords: *Squeezing Ground; Tunnel Collapse; Convergence Monitoring; Swelling Claystone; Ring Closure; Time-Dependent Deformation.*

How to Cite: Kaustubh Mani Nepal (2026) Delayed Ring Closure as the Primary Cause of Tunnel Collapse in Swelling Claystone: A Lesson from Jatigede Hydroelectric Power Project, Indonesia. *International Journal of Innovative Science and Research Technology*, 11(9), 744-752. https://doi.org/10.38124/ijisrt/26sep312

I. INTRODUCTION

The Jatigede Hydroelectric Power Project (110 MW) is a storage-type power project located on the Cimanuk River in Sumedang Regency, West Java, Indonesia. The project generates approximately 5 hours of electricity per day to meet the national grid's peak energy demand of 462.6 GWh, with a design discharge of 73 m^3/s. At present, the project is under commercial operation.

The penstock tunnel, the subject of this study, is a 731.54 m-long steel-lined pressure tunnel conveying water from the pressure shaft (elevation: 90 m) to the powerhouse (elevation: 68.25 m). The tunnel consists of: a. A transition segment measuring 4.5 m in length (with a diameter transitioning from 4.5 m to 4.0 m); b. A main pipe segment that is 693.54 m long (with a diameter of 4.5 m/4.0 m); c. Branch pipe segments measuring 31 m and 38 m (with diameters ranging from 3.5 m to 2.5 m).

II. METHODOLOGY

➢ *Geological Investigation*

The tunnel alignment traverses Pliocene volcanic breccia, conglomerate, and tuffaceous sandstone, as well as Miocene claystone.

ISSN No:-2456-2165 https://doi.org/10.38124/ijisrt/26sep312

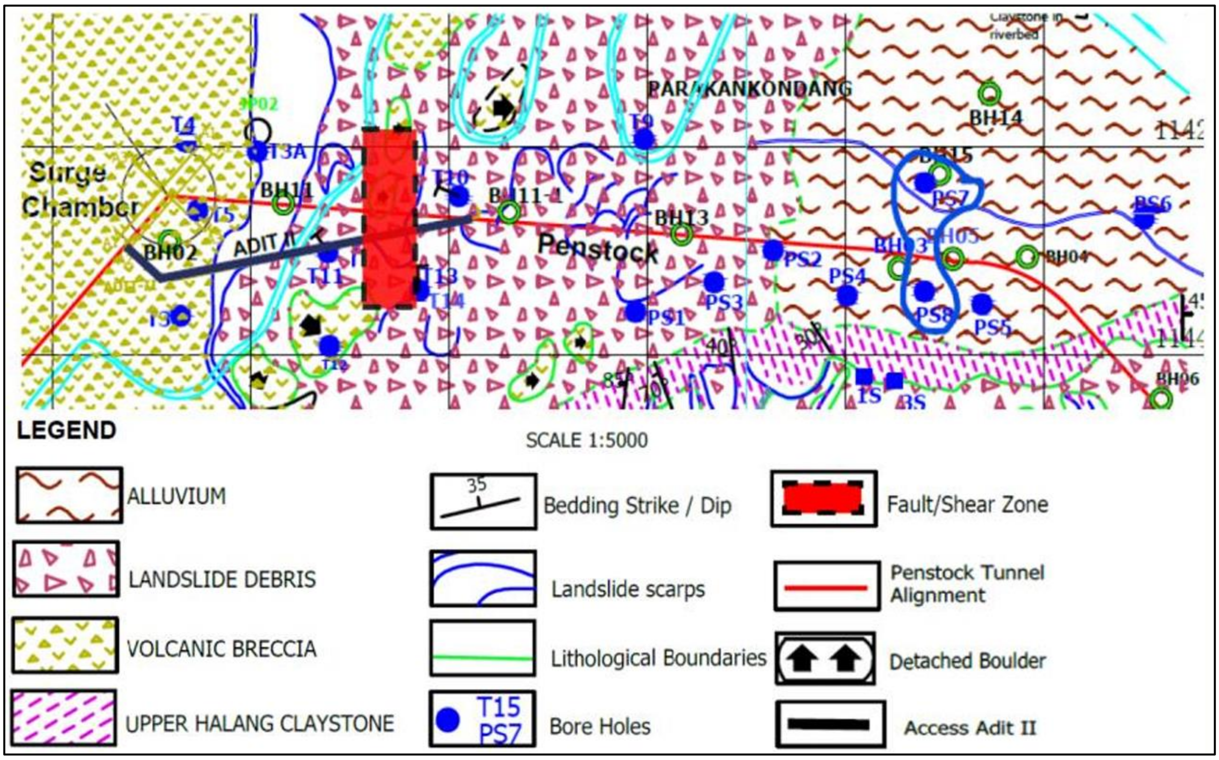

Fig 1 Location of Core-Drilled Investigation as well as Miocene Claystone [28, 29].

The boundary between the breccia and claystone is influenced by gravity-driven displacement and faulting, resulting in shearing in the claystone. The following key geological features were identified during feasibility studies:

- The tunnel (Ch. PS0+000 – 0+200 m) is located in volcanic breccia from the Pliocene era.
- From Ch. PS0+200 m to PS0+250 m, folded Miocene claystone is interspersed with tuffaceous sandstone and breccia.

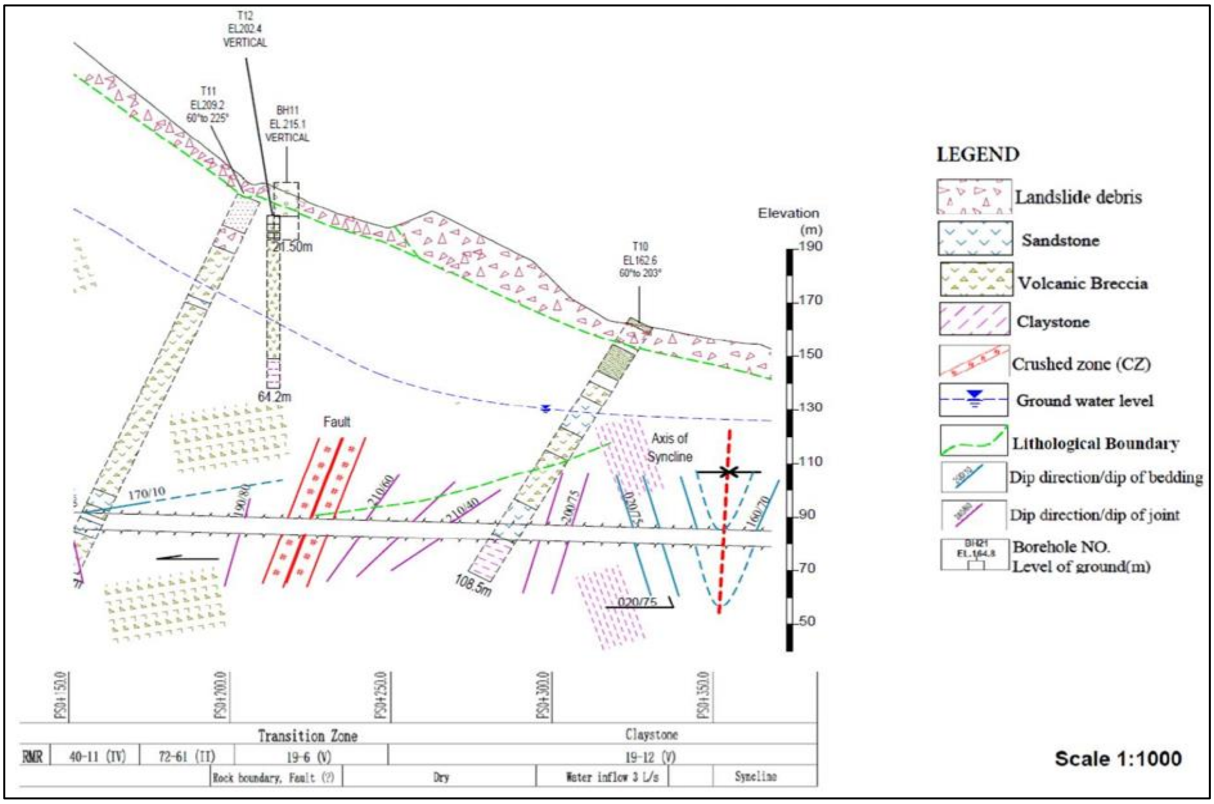

Fig 2 Longitudinal Geological Section Between Chainage PS0+395 and PS0+150.

ISSN No:-2456-2165 https://doi.org/10.38124/ijisrt/26sep312

- There is high permeability in the faulted layers of the Miocene and Pliocene.
- Between Ch. PS0+250 m and 0+731.54 m, the material consists of sheared, swelling claystone with low permeability.
- The depth of groundwater varies from 30 m to 130 m beneath the surface.

Fig 1 illustrates the locations of drilled investigation holes along the tunnel route. The as-built longitudinal geological section from Ch. PS0+395 to Ch. PS0+150 of the tunnel is presented in Fig 2.

The claystone exhibits characteristics indicative of challenging tunnelling conditions. The results for the physical and mechanical properties of clay samples collected and tested during the project study are also presented in Table 1 [23], [24].

Table 1 Summary of Geotechnical Parameters for the Claystone [23], [24].

Parameter	Value / Range	Remarks
Classification (USCS)	CH, MH	High to medium plasticity clay
Grain Size	86–100% finer than 0.075 mm	Fine-grained material
Dry Density (kN/m³)	18.0	–
Atterberg Limits		
• Liquid Limit (LL)	73% – 121%	–
• Plastic Limit (PL)	38% – 82%	–
• Plasticity Index (PI)	26% – 39%	–
Grain Specific Weight (G_s)	2.67 – 2.73	–
Shrinkage	14% – 23%	Significant shrinkage potential
Strength Parameters		
Undrained Shear Strength	0.35 – 5.7 MPa (Avg: 3.0 MPa)	Large variability
Unconfined Compressive Strength (UCS)	Stronger material: 2.7 – 13.9 MPa	Average from core tests: 0.8 MPa
	Weaker material: 1.3 – 4.8 MPa (Avg: ~1.6 MPa)	
Stiffness		
Modulus of Elasticity (E)	Stronger claystone: 310 – 400 MPa	Highly dependent on the rock mass condition
	Fractured/sheared claystone: 110 – 190 MPa	

During the pre-excavation stage, several critical observations were noted: the material has high plasticity, significant shrinkage potential, and variable strength and stiffness, which are greatly influenced by its state—whether intact or fractured/sheared [2], [3], [6]. It is characterised as a weak, highly plastic, swelling rock that is primarily composed of montmorillonite, along with minor amounts of kaolinite, pyrite, and gypsum.

The notable difference between high intact compressive strength (up to 13.9 MPa UCS) and low average core test strength (0.8 MPa) highlights the substantial impact of fractures and defects on overall behaviour. The physical and mechanical properties of the rocks used in the design are presented in Table 2.

During the construction period, the tunnel face after excavation was geologically logged and critically analyzed, and the rock's intact strength was verified by point-load testing of rock lump samples.

The adverse geological conditions described above necessitated rigorous deformation monitoring to quantify the ground response and evaluate support performance. The following section describes the monitoring program and analytical framework employed.

Table 2 Physical-Mechanical Parameters of the Rock Mass Class [18] Along the Tunnel Alignment Adopted During Design.

Rock Mass Class	**Rock Mass Type**	**Density, g/cm³**	**Shear strength**		**Deformation Modulus, GPa**	**Elastic Modulus, GPa**	**Poisson Ratio**	**Swelling Percent**	**Porosity Percent**
			Friction coefficient, f	**Cohesion, MPa**					
V	Highly Fractured / Sheared Claystone	1.8	0.28*	0.08*	0.25	0.4	0.4	37	46

*Note – Back-Calculated Values after Tunnel Collapse for Treatment.

ISSN No:-2456-2165 https://doi.org/10.38124/ijisrt/26sep312

➢ *Monitoring and Analysis Model*

Convergence data and curves were analyzed using the Sulem (1987) [1, 8, 11] time-dependent deformation model. This model provides insight into instantaneous convergence (C_{ox}), time-dependent creep ratio (m), and total asymptotic convergence.

The semi-empirical law proposed by Sulem et al. (1987) (Equation 1) allows the distinction between these two effects and is commonly used in the analysis of convergence data, where C_{ox} represents the instantaneous convergence obtained in the case of an infinite rate of face advance (no time-dependent effect), X is a parameter related to the distance of influence of the face, T is a parameter related to time-dependent properties of the system (rock mass – support), m is a parameter which represents the relationship between the long-term total convergence and the instantaneous convergence, and n is a form-factor which is often taken equal to 0.3:

$$C(x,t) = C_{\infty x}\left[1-\left(\frac{X}{x+X}\right)^2\right]\left\{1+m\left[1-\left(\frac{T}{t+T}\right)^n\right]\right\} \quad (1)$$

By fitting the convergence data to this law, the total long-term convergence can be obtained as:

$$C_{ox}(1+m) \quad (2)$$

III. RESULTS AND DISCUSSION

A. *Chronology of Failure*

Between October 2018 and June 2019, three major collapse incidents occurred due to groundwater inrush and roof instability in the studied tunnel sections. Additionally, on January 12, 2020, a significant incident of invert heaving was recorded, with a maximum heave of 60 cm observed over three days.

To understand the driving forces behind these failure incidents, the in-situ stress regime at the project site was evaluated, as described in the following section.

B. *In-Situ Stress Conditions*

The regional tectonic setting at the project site indicates a north-south-oriented compressive crustal stress, influenced by the nearby Sunda Trench [4]. The horizontal stress comprises gravity-driven and tectonic components, with the measured value of 2 MPa from a nearby project. This results in horizontal stress exceeding vertical stress, significantly affecting tunnel stability. The initial lateral earth pressure coefficient for fractured claystone is set at 1.33, indicating a 33% greater horizontal stress than vertical stress, which exerts substantial inward pressure on tunnel walls. In weak rock masses, the elevated horizontal stress can induce significant horizontal convergence and may interact with swelling forces, potentially overwhelming inadequate support systems [5], [7].

C. *Deformation Measurement and Analysis*

➢ *Monitoring Section Layout*

The figure below illustrates the layout of the monitoring sections used to assess the tunnel's convergence deformation. The layout of convergence deformation monitoring lines is shown in Fig 3.

➢ *Convergence Data Overview*

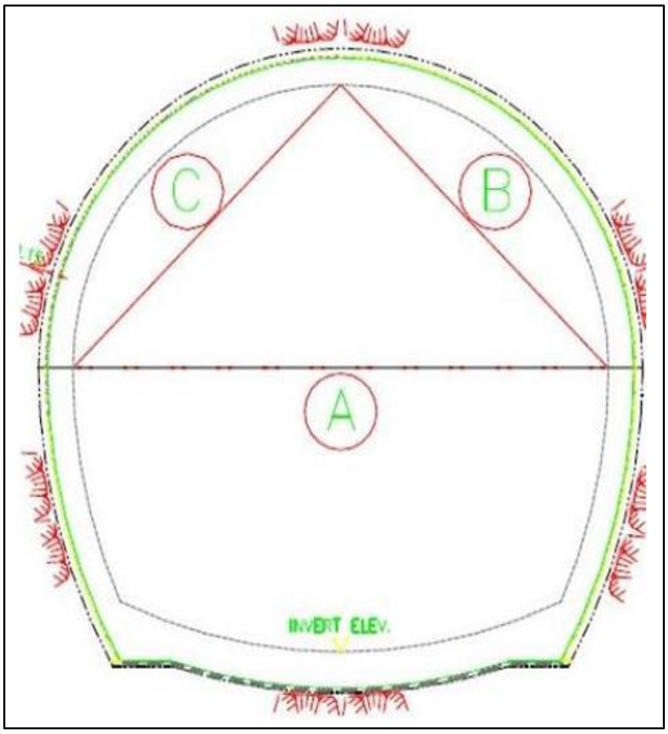

Fig 3 Layout of Convergence Deformation Monitoring Lines.

- Note: Line “A” was considered for this study of the monitoring section.

Convergence deformation monitoring data between PS0+395 and PS0+253 indicate significant deformation, particularly at PS0+330 and PS0+324, attributable to excavation challenges. The key observations are:

- Upward trend in deformation, indicating need for stronger support measures
- Before additional support at PS0+310: relative convergence reached 4.91%
- Daily deformation rates: 0.3–0.5 mm
- Resulting in invert heave and tunnel walls shotcrete cracking

The initial average convergence deformation observed along monitoring line A was 272.0 mm, corresponding to a closure percentage of 4.32%. After data processing, the average convergence deformation was 229.0 mm, corresponding to a closure percentage of 3.63%.

➢ *Analysis of Convergence Using the 'Sulem, 1987' Model*

The convergence curves were analysed using the Sulem (1987) [1], [14] time-dependent deformation model with:

ISSN No:-2456-2165 https://doi.org/10.38124/ijisrt/26sep312

- X = 10.5 m (fixed for all stations) [8], [9]
- n = 0.3 (fixed for all stations) [8], [9]

The values of X and n have been adopted from the Fréjus Road Tunnel [8], which serves as a reference example of a tunnel excavated in squeezing ground and exhibits time-dependent and anisotropic behaviour.

The model parameters provide insight into:

- Instantaneous convergence (C_ox)
- Time-dependent creep ratio (m)
- Characteristic time (T)
- Lost convergence (deformation before monitoring started)
- Total asymptotic convergence

➢ *Classification of Convergence Behaviour*

The convergence curves can be categorised into three behavioural types:

➢ *Group A: Severe, Very Severe Squeezing (PS0+290, PS0+303, PS0+324)*

- Behaviour: Enormous deformations exceeding 771 mm at PS0+324 and 197 mm at PS0+290. Curves show no signs of stabilisation during the monitoring period. High and continuous convergence rates. Deformations recorded after collapse treatment at PS0+290 [20]. A convergence curve for monitoring Station PS0+290 is shown below as a reference (Fig 4).

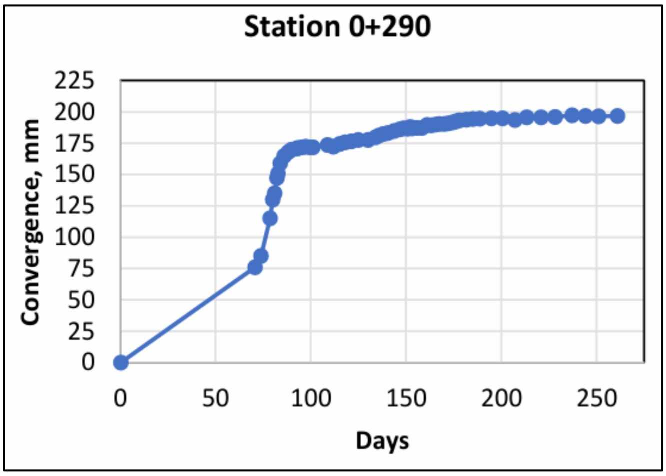

Fig 4 A Convergence Curve of Monitoring Station PS0+290.

- Interpretation: Classic sign of an overwhelmed support system. Rock mass strength insufficient to withstand redistributed stresses. Support (shotcrete, steel ribs) has yielded. Deformation combines plastic yielding and viscous creep.

- *Critical Findings:*

✓ PS0+324: Instantaneous convergence alone is 215 mm; total asymptotic convergence reaches 1,421 mm.
✓ PS0+303: m = 6.5 reflects extreme time-dependent deformation.
✓ PS0+290: m = 3.2 indicates long-term creep about three times the instantaneous part.

➢ *Group B: Variable Distances, Moderate to High Deformation, Persistent Creep (PS0+260, PS0+270, PS0+280, PS0+355)*

- Behaviour: Significant deformation (50–200 mm) but at a slower, steadier rate after initial rapid movement. The secondary creep phase is represented by a nearly straight line on the deformation-time graph. A convergence curve for monitoring Station PS0+260 is shown below as a reference (Fig 5).

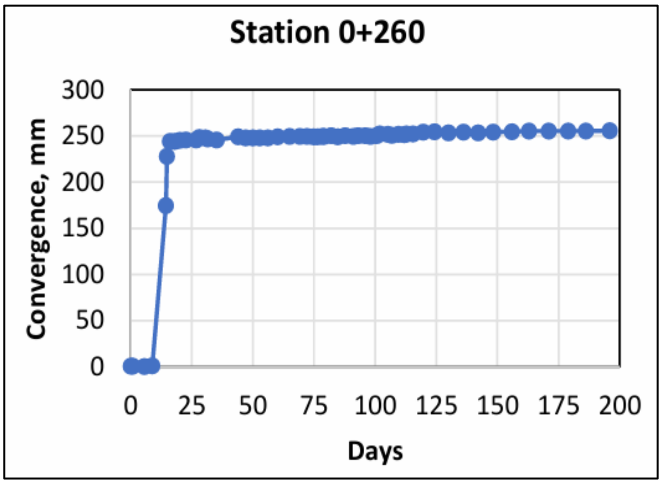

Fig 5 A Convergence Curve of Monitoring Station PS0+260.

- Interpretation: Hallmark of "Norton Power Law" in action. Rock mass undergoing steady-state, time-dependent deformation. Support system carrying load but neither stiff nor strong enough to arrest creep. A constant strain rate indicates that the deviatoric stress remains high enough to sustain continuous plastic flow.

- *Critical Findings:*

✓ PS0+260: Extremely short characteristic time (5 days) – time-dependent deformation occurs within a week.
✓ PS0+355: Very long characteristic time (200 days) – slow, persistent creep.
✓ PS0+270: Much less active section, indicating stable ground.

➢ *Group C: Limited, Stabilising Deformation (PS0+253, PS0+264, PS0+350, PS0+395)*

- Behaviour: Relatively small deformations (<25 mm at some stations). Curves flatten out (approaching asymptote) over time, indicating stabilisation. A convergence curve for monitoring Station PS0+253 is shown below for reference (Fig 6).

ISSN No:-2456-2165 https://doi.org/10.38124/ijisrt/26sep312

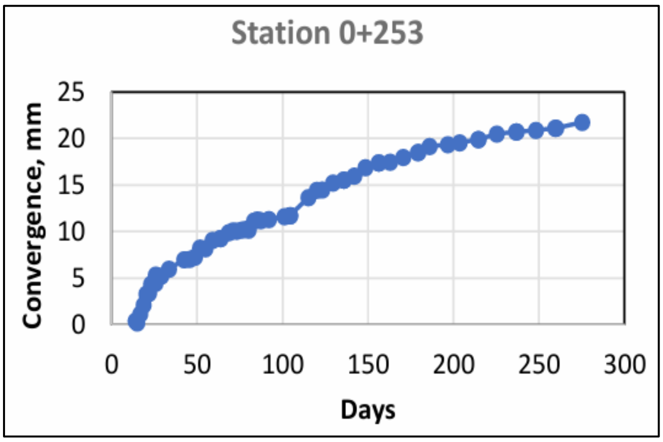

Fig 6 A Convergence Curve of Monitoring Station PS0+253.

- Interpretation: Sections in relatively more competent rock mass (higher RMR), subject to lower stresses, or benefited from more favourable local geology. Support system adequate to bring the ground to a new equilibrium.

- *Critical Findings:*

✓ PS0+264: Total convergence of 29 mm, the smallest among all stations.
✓ PS0+395: Low deformation of 31 mm over 500 days.
✓ PS0+350: Although located far behind, it still shows moderate deformation (280 mm total).

D. Summary of Sulem Model Parameters with Back-Calculated Convergence

The key parameters characterising each behavioural group are summarised in Table 3, which presents the back-calculated Sulem (1987) model parameters for all monitoring stations.

Table 3 Summary of Sulem Model Parameters with Back-Calculated Lost, Measured and Total Convergence for all Monitoring Stations.

Group	Station	C_ox (mm)	m	T (days)	Lost Convergence (mm)	Measured Convergence (mm)	Total Convergence (mm)	Behaviour Classification
A	PS0+290	55	3.2	35	0	197	197	Severe squeezing
A	PS0+303	80	6.5	30	282	262	544	Extreme squeezing
A	PS0+324	215	6.0	30	652	771	1,421	Extreme squeezing
B	PS0+260	100	5.0	5	246	253	499	Rapid squeezing
B	PS0+270	20	2.0	30	30	44	74	Moderate squeezing
B	PS0+280	45	3.5	25	66	137	203	Transitional
B	PS0+355	122	5.0	200	190	524	714	Slow persistent creep
C	PS0+253	20	2.0	40	17	24	41	Stable
C	PS0+264	12	1.8	80	0	29	29	Stable
C	PS0+350	55	3.2	35	123	157	280	Moderately stable
C	PS0+395	12	2.0	30	84	31	115	Stable

E. Correlation with Geological and Geotechnical Data

The tunnel was driven through claystone characterized by Rock Mass Rating (RMR) values primarily in Class V (Very Poor), ranging from 12 to 19. The Mohr-Coulomb parameters indicate a cohesion (c) of 80 kPa and an internal friction angle (φ) of approximately 15.6° [17], [18], a back-calculated value after collapse, suggesting an extremely weak rock mass comparable to very stiff soil [18]. A repeated collapse occurred at a location where the low-side cover was less than 1.5 times the excavated section, coinciding with a water accumulation zone following the October 2018 collapse. The material exhibits a swelling potential of 37%, primarily due to a high concentration of montmorillonite, which expands significantly when in contact with water. This swelling exerts considerable pressure on the support system and is a major contributor to long-term, time-dependent deformations [10], [13], [25]. In terms of in-situ stress, the horizontal-to-vertical stress ratio (K_o) is 1.33, indicating that horizontal stress is 33% greater than vertical stress, thereby exerting strong inward pressure on the tunnel walls in this weak rock mass [16], [8]. Furthermore, a significant initial water inflow of up to 18.5 L/s [16] had two detrimental effects: it softened the claystone, reducing its already low shear strength, and it initiated swelling in the montmorillonite clays, leading to long-term, time-dependent loads.

In addition to the primary support measures, cement grouting was implemented in the crown region to address ongoing deformation, as assessed in the following section.

F. Grouting Assessment

In response to the water inflow and to strengthen the collapsed and disturbed area, grout backfilling was adopted, and remedial grouting was carried out as follows: cement milk grouting was carried out in the crown region, specifically between PS0+300 and PS0+400 [16], where a hole approximately 1.7 meters deep was discovered in the rock. Following a 9-month observation period, the grouting proved effective only within this crown area. The injected cement grout was mixed with water at ratios of 2:1 and 1.3:1 and applied at a pressure of less than 1 MPa. This low pressure was meant to reduce stiffness and limit creep, but it failed to increase the rock mass stiffness enough to compensate for the missing rock bolts at the crown.

ISSN No:-2456-2165 https://doi.org/10.38124/ijisrt/26sep312

G. Analysis and Discussion

➢ *Critical Analysis of Construction Sequence and Support*

Despite extensive support, the construction methodology contained fatal flaws for these specific ground conditions.

➢ *The Fatal Flaw: Delayed Ring Closure*

Excavating the top heading for over 150 meters without closing the invert for more than 9 (nine) months significantly impacted the stability of the support structure. In soft, squeezing ground conditions, it is crucial to close the support ring—consisting of shotcrete, ribs, and invert—quickly to mobilize full ring capacity, ensure adequate bending and axial stiffness to withstand large pressures, and prevent the formation of a “hinge” at the haunches, which can result in excessive deformation and failure. Evidence of instability is documented in invert heave measurements of 200–400 mm on average, with a maximum of 600 mm, indicating an unstable base and an incomplete support ring, as the ground displaced the unconfined invert upwards.

➢ *Support System Inadequacies*

The congestion at the crown has prevented the installation of rock bolts because the fore-poling pipes, which are essential for creating a stabilised zone in the rock mass, are present. This lack of rock bolts effectively increases the burden on the steel ribs by enlarging the “arch” they must support, leaving the crown more vulnerable. Additionally, while canopy pipes and rebar fore-poling serve as necessary pre-support measures that primarily stabilise the face and the immediate excavation area, they cannot replace a robust, closed primary support ring behind the face.

➢ *Root Cause Scenario*

The sequence of events leading to the collapse and severe squeezing starts with excavation, which redistributes stress in the surrounding claystone. As the tunnel face advances, the weak rock cannot withstand the high horizontal stress. This results in stress-driven squeezing, causing the rock to deform plastically into the opening [5], [6], [7], [14], [19]. The primary support, consisting of ribs and shotcrete, is installed without a closed invert, functioning as an open horseshoe that lacks the required stiffness and capacity to withstand large, creeping pressures. As groundwater percolates into the ground, it causes montmorillonite in the clays to swell, which progressively increases the swelling pressure on the already high tectonic-driven stress; together, these factors contribute to tunnel deformation. This results in progressive failure of the support system, where ribs deform, shotcrete cracks, and tunnel convergence accelerates due to tertiary creep, while the invert heaves due to inadequate confinement. Eventually, at the weakest point (PS0+290, with an RMR as low as 12 and low cover at the left haunch of the tunnel crown), the cumulative deformation surpasses the capacity of the rock-support system, leading to collapse.

H. Interpretation of Deformation Behaviour

➢ *Time-Dependent Mechanisms*

The Sulem model parameters reveal three distinct time-dependent mechanisms of deformation. In the rapid creep phase ($T < 30$ days), stations located near the face or within highly fractured zones, such as PS0+260, PS0+280, PS0+303, and PS0+324, demonstrate rapid deformation development due to immediate plastic yielding and stress redistribution. Frenelus and Peng (2023) [10] reported more than 400 mm of creep convergence over 27 days in a similar deep, soft-rock tunnel, the Weilai Tunnel, comparable with the Jatigede asymptotic convergence of 1,421 mm noted at PS0+324.

This phase is followed by the persistent creep phase ($T =$ 30–80 days), during which most stations show moderate creep rates ($m = 2.0$–5.0). This behaviour indicates the inherent creep characteristics of the claystone under constant deviatoric stress [15]. Finally, in the slow creep phase ($T = 200$ days), station PS0+355, located well ahead of the collapse, shows very slow but persistent creep, indicating that the swelling process continues over extended periods.

To better understand the Jatigede experience and apply the lessons learned to future projects with similar ground conditions, the project's findings have been compared with observed behaviour in international tunnelling projects in difficult ground conditions.

➢ *Lost Convergence Significance*

The substantial loss of convergence values, reaching up to 652 mm at PS0+324, underscores the critical importance of early installation of monitoring. It indicates that a large portion of the deformation occurred before the monitoring sections were installed, with significant deformation also occurring immediately after excavation. Additionally, the delay in support installation relative to the face advance is a notable concern.

➢ *Comparison with Empirical Criteria*

- *Convergence Ratio:*

The maximum measured convergence was 4.91% prior to the addition of extra support, while the average convergence was 4.32% over a measurement of 272.0 mm. These figures notably exceed the typical design assumptions, indicating that the structural integrity may need to be reassessed.

- *Invert Heave:*

The maximum invert deformation measured is 600 mm, occurring over an extensive length of approximately 70 meters. This deformation clearly indicates inadequate confinement within the structure.

I. Lessons from International Practice

The international comparison confirms that the critical differentiator between success and failure in squeezing ground is not the type of support but the timing of installation. This finding is key to the conclusions and recommendations that follow [21], [24]:

ISSN No:-2456-2165 https://doi.org/10.38124/ijisrt/26sep312

Table 4 Comparison with Other Squeezing Ground Projects.

Project	Ground Conditions	Key Success Factor
St. Gotthard Base Tunnel	The “Piora Mulde” is a steep syncline filled with Triassic sedimentary rocks, including dolomites, anhydrite, gypsum, and greywacke – the tunnel’s biggest geological gamble. Weak rock, high overburden.	Immediate ring closure
Yacambu–Quibor Tunnel [26]	Severe plastic deformation from ultra-high tectonic stress in weak, highly foliated metamorphic rocks, exacerbated by multiple active shear faults.	Flexible support with yielding elements
Modaoren Tunnel	Complex geological challenges including high horizontal stress and faulted geology; thick layers of limestone, dolomite, sandstone, mudstone, shale, and thin coal seams, with high-pressure groundwater inrush.	Heavy steel ribs with close spacing
Jatigede (this case)	Swelling claystone, high horizontal stress.	Failed due to delayed ring closure

- Remarks: The main difference between success and failure in ground squeezing is not the type of support used, but the timing of its installation, especially the timing of invert closure [21].

IV. CONCLUSIONS AND RECOMMENDATIONS

The Jatigede Penstock Tunnel case highlights the challenges of tunnel construction in weak, swelling ground conditions. Key findings from the study include the identification of severe squeezing behaviour and three major collapse incidents, driven by convergence monitoring data and geological investigations. Three behavioural groups were observed:

- Group A: Experienced severe, unstable squeezing with significant convergence, indicating an inadequate support system.
- Group B: Showed moderate to high deformation with ongoing creep, revealing a support system that carried the load but lacked stiffness.
- Group C: Demonstrated limited, stabilizing deformation in a more competent rock mass, where the support was sufficient for stability.

The geological conditions were the main cause of instability in the tunnel, which passes through weak claystone classified as RMR Class V, with cohesion of 80 kPa and an internal friction angle of about 15.6°. This material has a swelling potential of 37% and a high porosity of 46%, largely due to montmorillonite, which expands when hydrated. Additionally, the in-situ stress conditions worsened the instability, having a horizontal-to-vertical stress ratio of 1.33, meaning horizontal stress was 33% greater than vertical stress. This combination of geological factors and high horizontal stress led to squeezing and swelling, ultimately compromising the support systems.

The weak geological conditions were critical to the catastrophic failure, particularly the prolonged delay in closing the support ring after 9 (nine) months of excavation over a distance of 150 meters. This late closure compromised the support system's integrity. In soft squeezing ground, promptly closing the support ring, which includes shotcrete, ribs, and invert, is essential to mobilize its full capacity and prevent excessive deformation. Evidence of instability was shown by invert heave measurements of up to 600 mm, indicating an unstable base and incomplete support ring. The inability to install rock bolts at the crown due to congestion further weakened the system. The failure was driven by stress-induced squeezing and inadequate support, resulting in collapse at the weakest point, where the rock mass rating was as low as 12.

The important lesson from this project is clear – in squeezing ground, it is not enough to install strong support; the support must be installed as a closed ring at the earliest possible moment. The timing of support installation is as critical as its strength. This case study also demonstrates the immense value of systematic convergence monitoring and its interpretation using analytical models such as Sulem (1987) to understand deformation mechanisms, identify developing instability, trigger appropriate intervention measures, and provide data for back-analysis and future design.

RECOMMENDATION

For future projects in similar ground conditions, it is strongly recommended to reduce the distance between top heading face and the completed invert to a maximum of 1–2 diameters, implement robust closed ring support from the outset with heavier steel sections and reduced rib spacing, ensure systematic rock bolting over the entire tunnel profile, and establish rigorous real-time monitoring with three-level alert thresholds to enable timely emergency responses. The lessons learned from the Jatigede Penstock Tunnel provide invaluable guidance for tunnel construction in weak, swelling rock masses worldwide and underscore that careful attention to construction sequence and timing is paramount to project success.

ACKNOWLEDGEMENTS

The authors acknowledge the contribution of all parties involved in the Jatigede Hydropower Project for providing access to monitoring data and geological information. The support of the project owners and construction team in documenting the failure mechanisms is gratefully appreciated.

ISSN No:-2456-2165 https://doi.org/10.38124/ijisrt/26sep312

REFERENCES

- [1]. Sulem, J., Panet, M., and Guenot, A. (1987). Closure analysis in deep tunnels. *International Journal of Rock Mechanics and Mining Sciences & Geomechanics Abstracts*, 24(3), 145-154.
- [2]. Bieniawski, Z. T. (1989). *Engineering Rock Mass Classifications*. Wiley-Inter-Science.
- [3]. Hoek, E., and Brown, E. T. (1997). Practical estimates of rock mass strength. *International Journal of Rock Mechanics and Mining Sciences*, 34(8), 1165-1186.
- [4]. World Stress Map (2016). *World Stress Map Database Release 2016*. GFZ Potsdam.
- [5]. Aydan, Ö., Akagi, T., & Kawamoto, T. (1993). The squeezing potential of rocks around tunnels: Theory and prediction. *Rock Mechanics and Rock Engineering*, 26(2), 137-163.
- [6]. Singh, B., and Goel, R. K. (2006). *Tunnelling in Weak Rocks*. Elsevier Geo-Engineering Book Series, Volume 5.
- [7]. Barla, G. (1995). Squeezing rocks in tunnels. *ISRM News Journal*, 2(3/4), 44-49.
- [8]. Manuel de la Fuente Mata. (2018). Tunnelling under squeezing conditions: Effect of the excavation method. *École Doctorale Sciences, Ingénierie et Environnement (SIE)*, Thèse de doctorat.
- [9]. Thakur, P. K. (2005). Analysis of Time-Dependent Response of Tunnels Considering Creep Effect. Asian Institute of Technology, School of Civil Engineering, Master of Engineering, Thesis.
- [10]. Frenelus, W., and Peng, H. (2023). Evaluating the Time-Dependent Behaviour of Deeply Buried Tunnels in Soft Rock Environments and Relevant Measures Guaranteeing Their Long-Term Stability. *Applied Sciences*, 13(18), 10542. https://doi.org/10.3390/app131810542.
- [11]. Barlow, J. P. (1986). Interpretation of Tunnel Convergence Measurements. Master Thesis, The University of Alberta, Department of Civil Engineering.
- [12]. Huang, J., Liu, X. W., et al. (2023). The stability evaluation of clay tunnels via the non-linear deterioration of physical and mechanical properties of surrounding rocks. *Frontiers in Geoscience*.
- [13]. Panthi, K. K. (2013). Predicting Tunnel Squeezing: A Discussion based on Two Tunnel Projects. *Hydro Nepal*, Issue 12, January 2013.
- [14]. Lee, C.H., Wang, T.T., Sun, L.J., and Huang, T.H. (2013). Invert heaving in operational tunnels – problems and countermeasures. In Proceedings of the World Tunnel Congress 2013 Geneva – Underground: The Way to the Future! (pp. 770–777). Taylor & Francis Group, London.
- [15]. Bonini, M., et al. (2009). The Mechanical Behaviour of Clay Shales and Implications for the Design of Tunnels. *Rock Mechanics and Rock Engineering*, 42, 361–388. DOI 10.1007/s00603-007-0147-6.
- [16]. Project Internal Report (2020). Submission of Completion Report on Water Inrush, Collapse, Mud Burst Penstock Tunnel PS0+290.
- [17]. Project Internal Report (2022a). Contractor Clarification on Tunnel Claims.
- [18]. Project Internal Report (2022b). Detailed Design Calculation and Analysis for the Surrounding Rock Stability of Penstock Tunnel from PS0+240m to PS0+390m (Rev. A).
- [19]. Steiner, W. (2000). Squeezing rock in Tunnelling: Identification and Important Factors. *Rivista Italiana Di Geotecnica*, 1/2000.
- [20]. Project Internal Report (2022c). Treatment of Serious Deformation at Penstock Tunnel.
- [21]. Gall, V., and Pyakurel, S., et al. (2017). Conventional Tunnelling in Difficult Ground. Proceedings of the World Tunnel Congress 2017 – Surface challenges – Underground solutions. Bergen, Norway.
- [22]. Jatigede Hydroelectric Power Plant, Tender Design Report. Xibei Engineering Corporation, China. September 2013.
- [23]. Jatigede Multi-Purpose Dam Project, Criteria and Basic Design Report Vol 1. (1986). Snowy Mountains Engineering Corporation (SMEC), Australia in Association with Indra Karya, Cirebon, Indonesia.
- [24]. Shimamoto, K., Yashiro, K., and Kawagoe, T. (2022). Floor heave and Effect of countermeasure for Mountain Tunnels. *Quarterly Reports of Railway Technical Research Institute*, RTRI Vol. 63-2, pp. 115-120.
- [25]. Saroglou, C. (2025). The Challenge of Rock Mass Classification of Anisotropic Rock Masses. *Rock Mechanics and Rock Engineering*. https://doi.org/s00603-025-04681-8.
- [26]. Hoek, E., and Guevara, R. (2009). Overcoming Squeezing in the Yacambú-Quibor Tunnel, Venezuela. *Rock Mechanics and Rock Engineering*, 42(2), 389-418. DOI:10.1007/s00603-009-0175-5.